

## On The Function $D(s)$ Associated With Riemann Zeta Function

Zarema S. Seidametova<sup>1</sup>, Valerii A. Temnenko<sup>2</sup>

<sup>1</sup>Department of Applied Informatics, Crimean Engineering-Pedagogical University, Simferopol, Crimea

<sup>2</sup>Department of Applied Informatics, Crimean Engineering-Pedagogical University, Simferopol, Crimea

**Abstract :** We consider the function  $D(s)$  of the complex argument  $s=\sigma+it$ , formed with the use of a certain procedure of a transition to the limit. For  $\sigma>1$  the function  $D$  reduces to the Riemann zeta function, multiplied by the factor  $(s-1)$ . For  $\sigma<1$  the function  $D$  is a constant. For  $\sigma=1$  function  $D$  is undefined. A numerical investigation of  $D(s)$  for  $\sigma>1$  is presented. "Zeta effect" was discovered-the formation of fictitious short-period oscillations  $D(s)$ , caused by the confinement of a finite number of terms in the summation of Riemann series containing a large number of harmonics with a slowly varying frequency. A procedure for the numerical suppression of these zeta oscillations is proposed. On the line  $\sigma=1$ , where  $D(s)$  is undefined, an infinite family of "Riemann functions", genetically related to the Riemann zeta function, is introduced. A numerical investigation of these "Riemannian curves" is presented.

**Keywords :** Riemann zeta function, the family of Riemannian curves, zeta effect.

### I. Introduction. D-Function Definition

Let us consider the function  $D(s)$  of the complex argument  $s=\sigma+it$ , defined by the expression:

$$D(s) = (1-s) \lim_{N \rightarrow \infty} \left( \frac{1}{N^{1-s} - 1} \cdot \sum_{n=1}^N \frac{1}{n^s} \right). \quad (1)$$

It is obvious that for  $\sigma > 1$  the limit of the sum in (1) turns into the Riemann zeta function, and, accordingly:

$$D(s) = (s-1)\zeta(s), \quad (\text{Re } s > 1). \quad (2)$$

Where  $\zeta(s) = \sum_{n=1}^{\infty} \frac{1}{n^s}$  is Riemann zeta function.

It is convenient to rewrite the formula (1) in the left half-plane ( $\text{Re } s < 1$ ) in the following equivalent form:

$$D(s) = (1-s) \lim_{N \rightarrow \infty} \left( \frac{1}{N} \cdot \sum_{n=1}^N \left( \frac{N}{n} \right)^s \right). \quad (3)$$

Formulas (3) and (1) are equivalent in the sense that the results of the limiting transition in both formulas are the same.

For large  $N$  the sum in formula (3) is approximated by the integral:

$$\sum_{n=1}^N \left( \frac{N}{n} \right)^s = N \cdot \int_0^1 x^{-s} dx + O(1) \quad (N \gg 1). \quad (4)$$

Consequently,

$$\lim_{N \rightarrow \infty} \left( \frac{1}{N} \cdot \sum_{n=1}^N \left( \frac{N}{n} \right)^s \right) = \frac{1}{1-s}, \quad (5)$$

and, therefore,

$$D(s) \equiv 1 \quad (\text{Re } s < 1). \quad (6)$$

Therefore, the function  $D(s)$ , defined by formula (1) in the entire complex plane (with the exception of the straight line  $\sigma=1$ ), in the right-hand half-plane ( $\sigma>1$ ) in accordance with formula (2) differs from the Riemann zeta function only by the factor  $(1-s)$ , and in the left half-plane, in accordance with formula (6), it is

equal to one. Formula (1), in a certain sense, extends the Riemann series  $\sum_{n=1}^{\infty} n^{-s}$  to the entire complex plane  $s$

(except for the straight line  $\sigma=1$ ). This extension has a less elegant form than the well-known Riemann functional equation relating  $\zeta(s)$  and  $\zeta(1-s)$  (see, for example, Eq. 23.2.6 in the handbook [1]). However, this

extension (1) has also the right to exist.

It is convenient to divide the real and imaginary parts of the function  $D$ :

$$D(s) = R(\sigma, t) + iI(\sigma, t) \tag{7}$$

where

$$\left. \begin{aligned} R(\sigma, t) &= t \cdot B(\sigma, t) + (\sigma - 1)A(\sigma, t), \\ I(\sigma, t) &= t \cdot A(\sigma, t) - (\sigma - 1)B(\sigma, t), \end{aligned} \right\} \tag{8}$$

$A$  and  $B$  are the real Riemann series:

$$\left. \begin{aligned} A(\sigma, t) &= \lim_{N \rightarrow \infty} \sum_{n=1}^N \frac{\cos(t \ln n)}{n^\sigma}, \\ B(\sigma, t) &= \lim_{N \rightarrow \infty} \sum_{n=1}^N \frac{\sin(t \ln n)}{n^\sigma}. \end{aligned} \right\} \tag{9}$$

It follows from (9) that the series  $A(\sigma, t)$  and  $B(\sigma, t)$  have very simple asymptotics for large values of  $\sigma$ :

$$\left. \begin{aligned} A(\sigma, t) &\rightarrow \infty, \\ B(\sigma, t) &\rightarrow 0, \end{aligned} \right\} \sigma \rightarrow \infty.$$

Consequently, in accordance with formulas (8), the asymptotics of  $D(s)$  for  $\sigma \rightarrow \infty$  and fixed  $t$  has the following form:

$$\left. \begin{aligned} R(\sigma, t) &\cong \sigma - 1, \\ I(\sigma, t) &\cong t. \end{aligned} \right\}$$

Curiously, for  $t=0$  the real function  $D(\sigma)$  is continuous for all  $\sigma$  ( $-\infty < \sigma < +\infty$ ), including the point  $\sigma=1$  (see Figure 1), in spite of the singularity of the zeta function at this point.

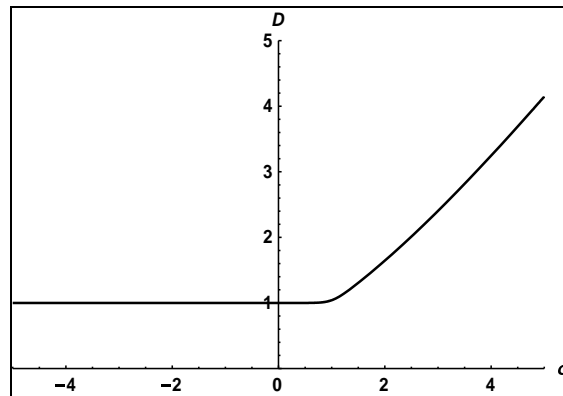


Fig.1. The function  $D$  for a real argument  $\sigma$ .

## II. A Rate Of Convergence Of The Riemann Series

To control the rate of convergence of the series (9), one can use expression (3), which determines the function  $D(s)$  in the left half-plane ( $\sigma < 1$ ). Separating the real and imaginary parts in formula (3), we can obtain the following relations:

$$D(s) \cong 1 = R(\sigma, t) + iI(\sigma, t),$$

where

$$\left. \begin{aligned} R(\sigma, t) &= (1 - \sigma) \cdot F(\sigma, t) + t \cdot G(\sigma, t), \\ I(\sigma, t) &= (1 - \sigma) \cdot G(\sigma, t) - t \cdot F(\sigma, t), \end{aligned} \right\} \tag{10}$$

$F$  and  $G$  are the real Riemann series

$$\left. \begin{aligned} F(\sigma, t) &= \lim_{N \rightarrow \infty} \left[ \frac{1}{N} \cdot \sum_{n=1}^N \left( \frac{N}{n} \right)^\sigma \cdot \cos \left( t \ln \frac{N}{n} \right) \right], \\ G(\sigma, t) &= \lim_{N \rightarrow \infty} \left[ \frac{1}{N} \cdot \sum_{n=1}^N \left( \frac{N}{n} \right)^\sigma \cdot \sin \left( t \ln \frac{N}{n} \right) \right]. \end{aligned} \right\} \tag{11}$$

For the calculations of  $F$  and  $G$  it is convenient to use not formulas (11), but finite approximations

(11) for sufficiently large  $N$  without the limiting transition  $N \rightarrow \infty$  :

$$\begin{aligned}
 F(\sigma, t) &\Rightarrow F_N(\sigma, t) = \frac{1}{N} \cdot \sum_{n=1}^N \left(\frac{N}{n}\right)^\sigma \cdot \cos\left(t \ln \frac{N}{n}\right), \\
 G(\sigma, t) &\Rightarrow G_N(\sigma, t) = \frac{1}{N} \cdot \sum_{n=1}^N \left(\frac{N}{n}\right)^\sigma \cdot \sin\left(t \ln \frac{N}{n}\right).
 \end{aligned}
 \tag{12}$$

( $\sigma < 1; N \gg 1$ ).

Calculating  $R(\sigma, t)$  and  $I(\sigma, t)$  for  $\sigma < 1$  by formulas (10) and using their approximations (12) instead of  $F$  and  $G$  (11), one can get an idea of the accuracy of calculating the function  $D(s)$ .

These calculations show that if the  $N$  terms of the series are kept in the sums (12) of the series, the deviations  $\Delta \varepsilon$  for  $R$  and  $I$  from the correct values  $R = 1$  and  $I = 0$  are of the order of  $1/N$  for  $N > 10^4$  for  $\sigma = -1$  and  $|t| < 1$ . These deviations slowly increase with increasing  $|\sigma|$  and  $|t|$  for fixed  $N$ . In the strip  $0 < \sigma < 1, t \neq 0$ , formulas (10) and (12) give an excessively large error in the calculation of  $D(s)$  for  $N \leq 10^6$ .

### III. Using A Finite-Dimensional Approximation Of The Riemann Series

When calculating the function  $D(s)$  in the right half-plane of the complex argument  $s$  (for  $\sigma > 1$ ) we also used finite-dimensional approximations of the oscillating real Riemann series (9). Instead of formulas (9) containing the limiting transition  $N \rightarrow \infty$ , we used finite sums:

$$\begin{aligned}
 A_N(\sigma, t) &= \sum_{n=1}^N \frac{\cos(t \ln n)}{n^\sigma}, \\
 B_N(\sigma, t) &= \sum_{n=1}^N \frac{\sin(t \ln n)}{n^\sigma}.
 \end{aligned}
 \tag{13}$$

When computing the sums  $A_N$  and  $B_N$  we usually fix  $N$  in the range between  $N = 10^5$  and  $N = 10^6$ . A calculation with a smaller value of  $N$  introduced noticeable distortions in the results. Computations with large values  $N$  required an unacceptably high time consuming result. For  $N$  in the range  $10^5 - 10^6$  one calculation, – for example, plotting the dependence of  $R(t)$  for fixed  $\sigma$  and  $0 \leq t \leq 50$  – requires, depending on  $\sigma$  and  $N$  from several tens of minutes to several work hours for Mathematica 10.4. It should be noted that the well-known article of J.M. Borwein, D.M. Bradley and R.E. Crandall [2], giving an extensive review of the algorithms for calculating the Riemann zeta function, does not mention at all the "frontal" method that we used in this paper: the use of finite sums of Riemann series (9) while retaining a very large number of terms. Perhaps ignoring this method in [2] is due to its considerable computational complexity.

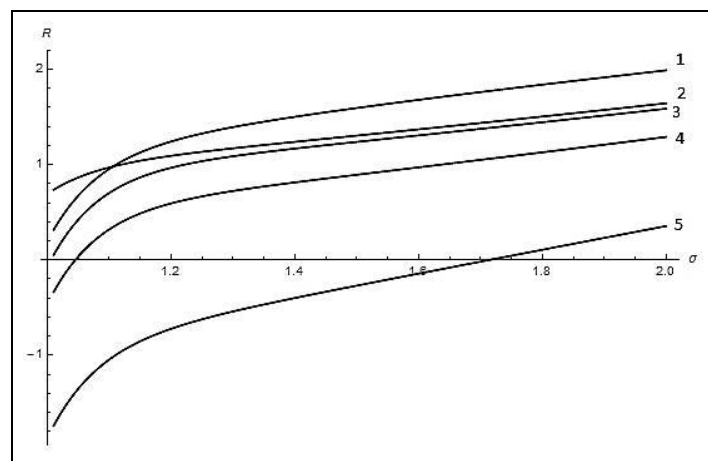


Fig.2. The  $R$ -function as the function of the argument  $\sigma$  for some values of the argument  $t$  (1 –  $t=10$ , 2 –  $t=0.1$ , 3 –  $t=1$ , 4 –  $t=2.5$ , 5 –  $t=5$ ).

Calculation by formulas (8) and (13) shows that the dependence of the functions  $R$  and  $I$  on the argument  $\sigma$  for a fixed value of the argument  $t$  is very simple and monotonic – see Fig. 2 and Fig. 3, which illustrate the dependence of  $R(\sigma)$  and  $I(\sigma)$  for several values of the argument  $t$  in the interval  $1 < \sigma \leq 2$ . For

$\sigma > 2$  functions  $R(\sigma)$  and  $I(\sigma)$  quite quickly "go out" to their asymptotic behavior for  $\sigma \rightarrow \infty$ .

The dependence of the functions  $R$  and  $I$  on the argument  $t$  (for a fixed value of the argument  $\sigma$ ) is much more complicated. These dependences contain exquisite and almost unpredictable oscillations with a characteristic interval of oscillations with respect to the argument  $t$  of order ten and a slowly increasing oscillation amplitude with increasing  $t$  (see Fig. 4, illustrating the dependence of  $R$  on  $t$  for  $\sigma=1.05$ ). Let us call them " $t$ -oscillations".

Corresponding  $t$ -oscillations of the Riemann zeta function can be seen in the pages of the old classical reference books on special functions – see, for example, Section VIII "Riemann zeta-function" in [3].

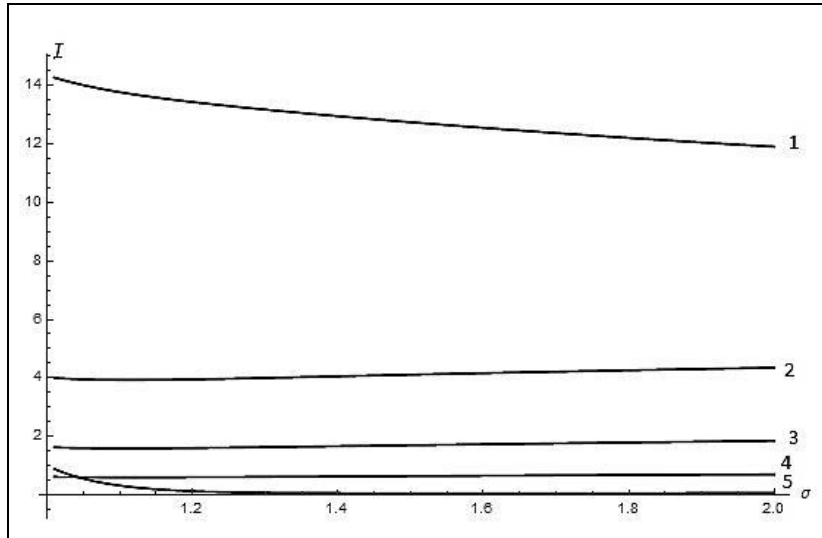


Fig.3. The  $I$ -function as the function of the argument  $\sigma$  for some values of the argument  $t$  ( $1 - t=10, 2 - t=5, 3 - t=2.5, 4 - t=1, 5 - t=0.1$ ).

#### IV. A Zeta Effect

But Fig. 4 demonstrates, in addition to real "slow"  $t$ -oscillations of sufficiently large amplitude, also the presence of an interesting effect of short-period "parasitic" oscillations of small amplitude. This effect (we called it the "zeta effect") is generated by a sharp break in the Riemann series (9) for a finite (albeit sufficiently large) value of  $n$ , equal to the "cut-off parameter"  $N \approx 10^5 - 10^6$ . In Fig. 4, these zeta oscillations significantly deform the dependence  $R = R(t)$  up to  $t \approx 15$ , but are also noticeable at  $t > 15$ .

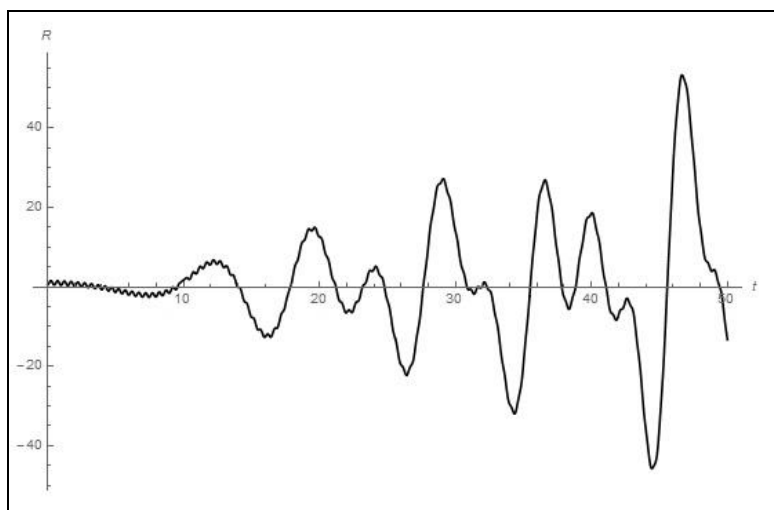


Fig.4. The  $R$ -function as the function of the argument  $t$  for  $\sigma=1.05$  ( $N=6 \cdot 10^5$ ).

We could not build an exact mathematical theory of the "zeta effect." However, it is not difficult to give a qualitative description of the causes of this phenomenon. The Riemannian finite sums (13) for a large value of the parameter  $N$  contain a large number of harmonics with a slowly varying frequency  $\omega_n = \ln n$  –

since for sufficiently big  $n$   $\ln n$  is a sufficiently slowly varying function. The highest oscillation frequency  $\omega_N$  is equal to  $\ln N$ . This frequency corresponds to a period of oscillations in the argument  $t$  is equal to  $T_N = 2\pi / \ln N$ . Accordingly, the characteristic period of these parasitic zeta oscillations is  $T_N \cong 0.50$  for  $N = 3 \cdot 10^5$  and  $T_N \cong 0.47$  for  $N = 6 \cdot 10^5$ . Fig. 5 illustrates this parasitic zeta-oscillation for the function  $I(t)$  for small ( $t \leq 1$ ), where this effect is most noticeable. Fig. 5 shows result of the calculation of the function  $I(t)$  for  $\sigma=1.01$  for three values of  $N$ :  $N = 3 \cdot 10^5; 4 \cdot 10^5; 6 \cdot 10^5$ . Judging from this figure, the characteristic time  $\Delta t$  of zeta-oscillations is somewhat less than the qualitative estimate of  $T_N$ , given by us, but coincides with this estimate in order of magnitude. This figure also shows the expected weak (logarithmic) decrease of  $\Delta t$  with increasing  $N$ .

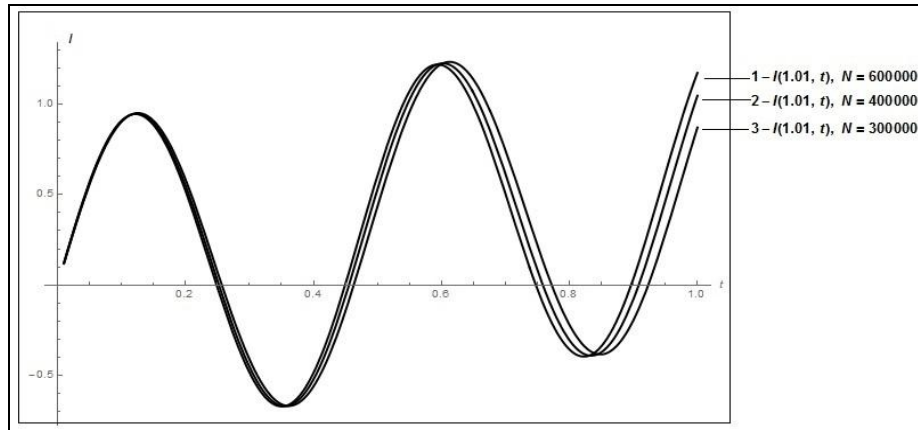


Fig.5. Zeta-oscillations of the function  $I(t)$  for  $\sigma=1.01$ .

One can give some rather crude estimate of the amplitude of these parasitic zeta oscillations. The contribution of one harmonic (that is, one summand in the sums (13)) to the amplitude for  $n$ , close to  $N$ , is of the order  $o(N^{-\sigma})$ . This is the "lower bound". The total number of harmonics in these sums with a low-varying frequency is very large for large  $N$  – because of the slow variation of the frequency  $\omega_n$ . As the "upper bound" for the number of these harmonics, one can take  $O(N)$ . The product of these two estimates gives a certain estimate (uncertain in its statistical status) for the amplitude of the zeta-oscillations:  $o(N^{-(\sigma-1)})$ . Accordingly, parasitic zeta oscillations show themselves especially strongly at small  $\sigma$ , close to the minimum permissible value  $\sigma=1$ .

In accordance with this estimate, for  $N = 10^5 - 10^6$  the amplitude of zeta oscillations at  $\sigma=1.01$  is a quantity on the order of unity. Fig. 5 gives a good confirmation of this rough estimate. As the  $\sigma$  increases, the amplitude of the zeta oscillations decreases rapidly for such  $N$ . At  $\sigma=2$  the zeta oscillations go to the fifth to the sixth digit after the decimal point, and with further increase  $\sigma$  become generally insignificant, drowning in the error of machine rounding of numbers.

How can we suppress these parasitic zeta-oscillations generated by the termination of infinite Riemann series (8)?

### V. An exponential $\beta$ -Damping

To suppress the zeta effect, we used "exponential  $\beta$ -damping", replacing each term in the Riemann sums (13) with its "damped" expression:

$$\left. \begin{aligned} A_N(\sigma, t) &\rightarrow A_{N,d}(\sigma, t, \beta) = \sum_{n=1}^N \frac{\cos(t \ln n)}{n^\sigma} e^{-\beta \frac{n}{N}} \\ B_N(\sigma, t) &\rightarrow B_{N,d}(\sigma, t, \beta) = \sum_{n=1}^N \frac{\sin(t \ln n)}{n^\sigma} e^{-\beta \frac{n}{N}} \end{aligned} \right\} \quad (14)$$

Where  $\beta$  is the damping parameter:  $\beta > 1$ . (In the calculations, we used the value  $\beta=5$ ).

Exponential  $\beta$ -damping (14) does not significantly affect the contribution of the majority of "low-frequency" harmonics with  $n \ll N$  and substantially reduces the contribution of terms with large numbers  $n$ , approaching to  $n=N$ . This method smoothes out the effect of a sharp break in the Riemann series (8) for  $n=N$ .

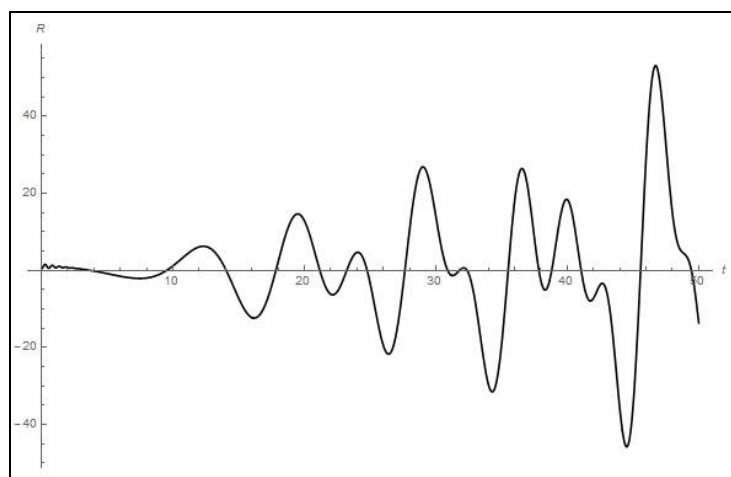


Fig.6. The dependence of the function  $R$  of argument  $t$  for  $\sigma=1.05$  ( $N=6 \cdot 10^5$ ). The dependence is calculated using the exponential  $\beta$ -damping procedure described in the article for  $\beta=5$ .

Fig. 6 demonstrates the effect of exponential  $\beta$ -damping on the numerical results of calculating the function  $D(s)$ . This figure shows the same graph shown earlier in Fig. 4: dependence of the function  $R$  on the argument  $t$  for  $\sigma=1.05$  and  $N = 6 \cdot 10^5$ . In Fig. 6 this dependence is calculated by the formulas (14), taking into account  $\beta$ -damping ( $\beta=5$ ). The "smoothed" function  $R(t)$  in this figure completely repeats the function  $R(t)$  of Fig. 4 in all that concerns real large-scale slow oscillations, but is practically free of parasitic oscillations generated by the zeta effect. The trace of these parasitic oscillations remained only for small  $t$  ( $t < 1$ ). The suppression of the zeta-effect in the region of small  $t$  requires an increase in the damping parameter  $\beta$ . An increase in  $\beta$  can cause distortion in real large-scale oscillations of the function  $R(t)$ . Here, the researcher must compromise, determining what is more important in a particular task – total suppression of the zeta-effect at small  $t$  or preservation of correct results for large  $t$ .

## VI. Graphical Representation Of Some Results For D-Function

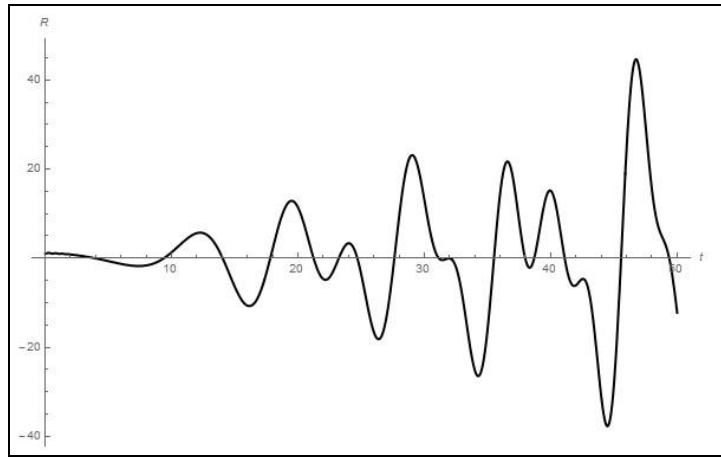
All further graphs of the functions  $R(t)$  and  $I(t)$  are represented by means of "smoothed" Riemann sums (14).

Figure 7 shows the dependence of the function  $R$  on the argument  $t$  for some values of the argument  $\sigma$ .

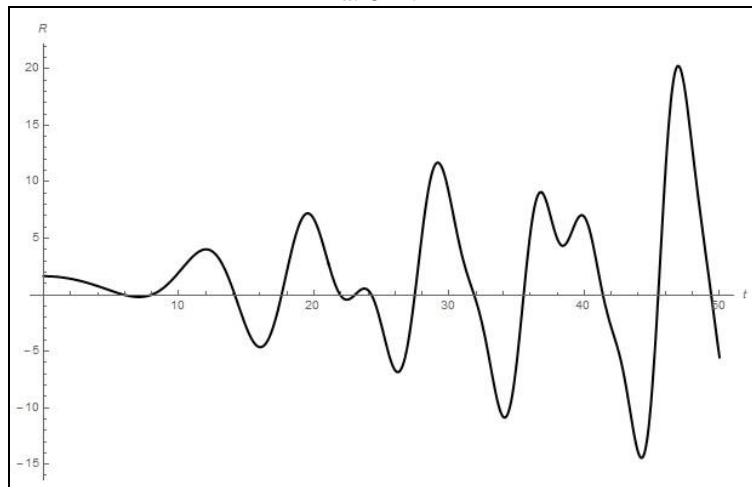
Figure 8 shows the dependence of the function  $I$  on the argument  $t$  for some values of the argument  $\sigma$ .

It can be seen from these figures that as the argument  $\sigma$  increases, the amplitude of the  $t$ -oscillations decreases.

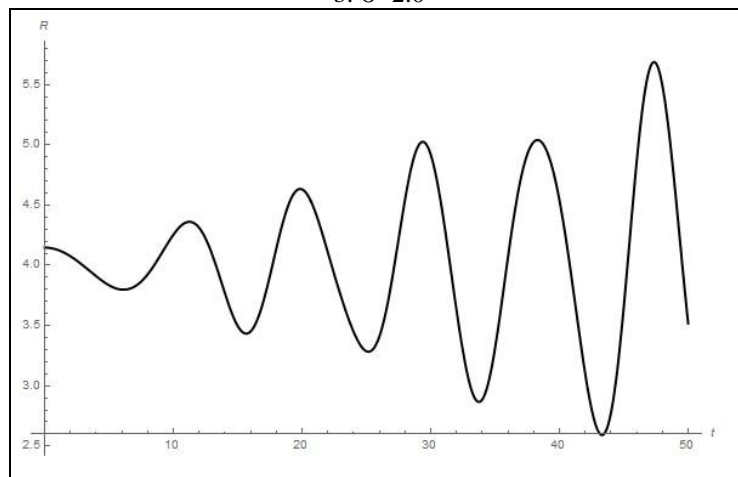
The pair of functions  $R(t)$  and  $I(t)$  in the complex plane of the function  $D(s)$ , given by equation (1) determines the isoline of the constant values of the argument  $\sigma$  (the real part of the complex argument  $s$ ). These curves are shown in Fig. 9 for different values of  $\sigma$  and values of  $t$  in the interval  $0 \leq t \leq 10$ . The loops seen in the initial part of the curves in Fig. 9a and Fig. 9b are fictitious. They reflect the zeta-oscillation unsuppressed for small  $t$ . Figures 9c and 9d correspond to large values of the argument  $\sigma$  at which the zeta effect does not manifest itself at small  $t$ .



a:  $\sigma=1.2$

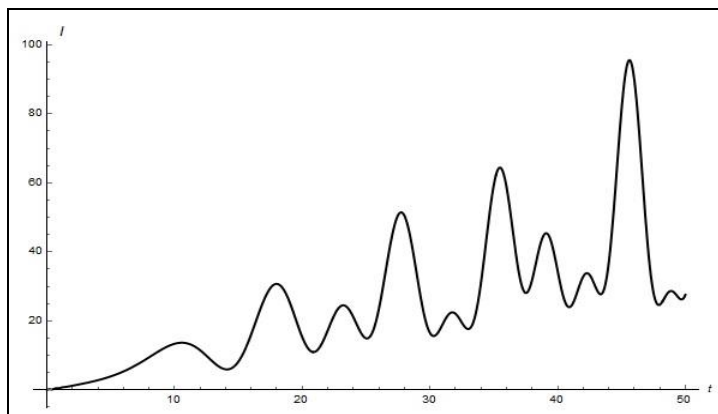


b:  $\sigma=2.0$

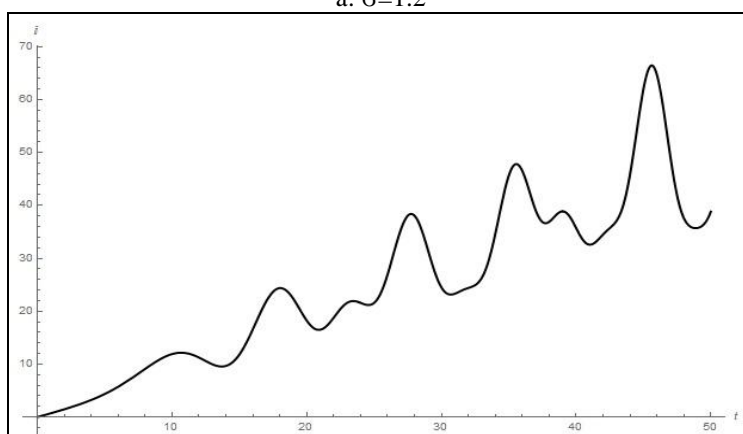


c:  $\sigma=5.0$

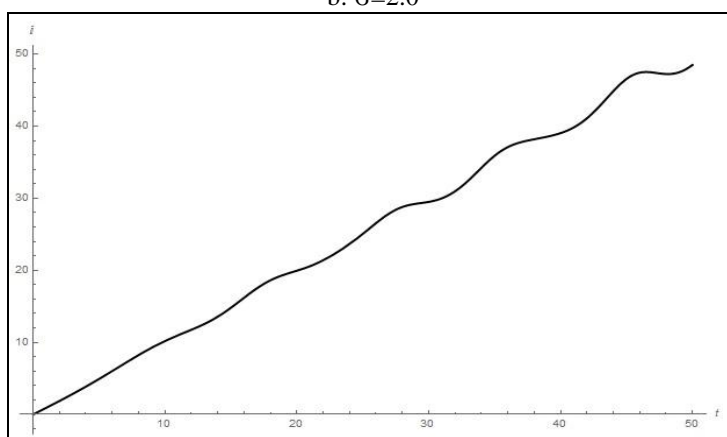
Fig. 7. The  $R$ -function as a function of argument  $t$  for some values of argument  $\sigma$ .



a:  $\sigma=1.2$

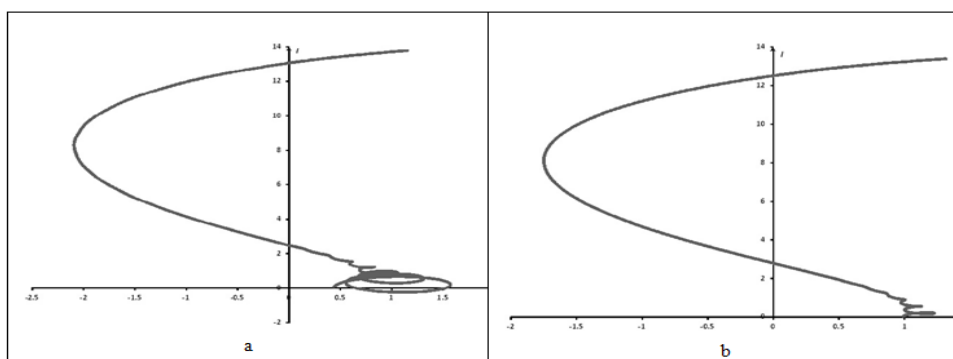


b:  $\sigma=2.0$



c:  $\sigma=5.0$

Fig. 8. The  $I$ -function as a function of argument  $t$  for some values of argument  $\sigma$ .



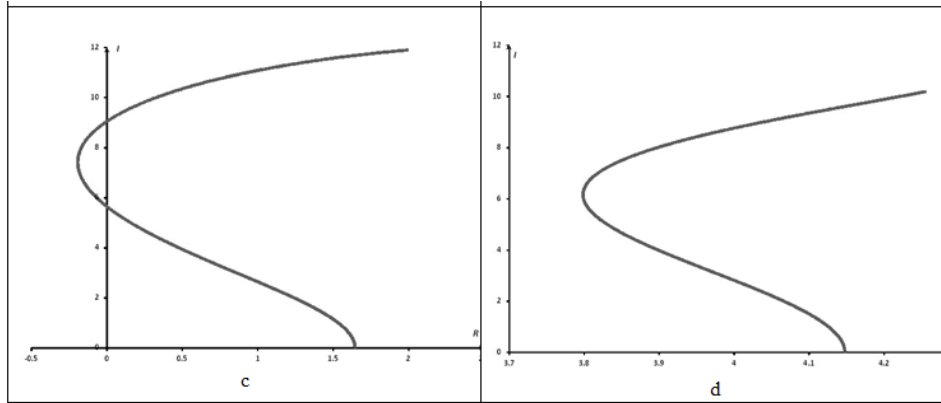


Fig. 9. The isolines of the constant values of argument  $\sigma$  in complex  $D$ -plane.  
 a:  $\sigma=1.05$ ; b:  $\sigma=1.2$ ; c:  $\sigma=2.0$ ; d:  $\sigma=5.0$

### VII. Constructing A Riemann Family Of Curves For $\sigma=1$

On the line  $\sigma=1$  the function  $D(s)$  is undefined: in the formula (1) for  $\sigma=1$  and  $t \neq 0$  there is no limit as  $N \rightarrow \infty$ . If in formula (1) we abandon the limiting transition  $N \rightarrow \infty$ , then formula (1) allows us to determine for  $\sigma=1$  some infinite family of plane curves  $x_N = x_N(t)$ ,  $x_N = \{x_N, y_N\}$ ,  $N \geq 3$ , where

$$x_N(t) = \frac{t}{2 \sin\left(\frac{1}{2}t \ln N\right)} \cdot \sum_{n=1}^N \frac{\sin\left(t \ln \frac{n}{\sqrt{N}}\right)}{n}, \quad (15)$$

$$y_N(t) = \frac{t}{2 \sin\left(\frac{1}{2}t \ln N\right)} \cdot \sum_{n=1}^N \frac{\cos\left(t \ln \frac{n}{\sqrt{N}}\right)}{n}$$

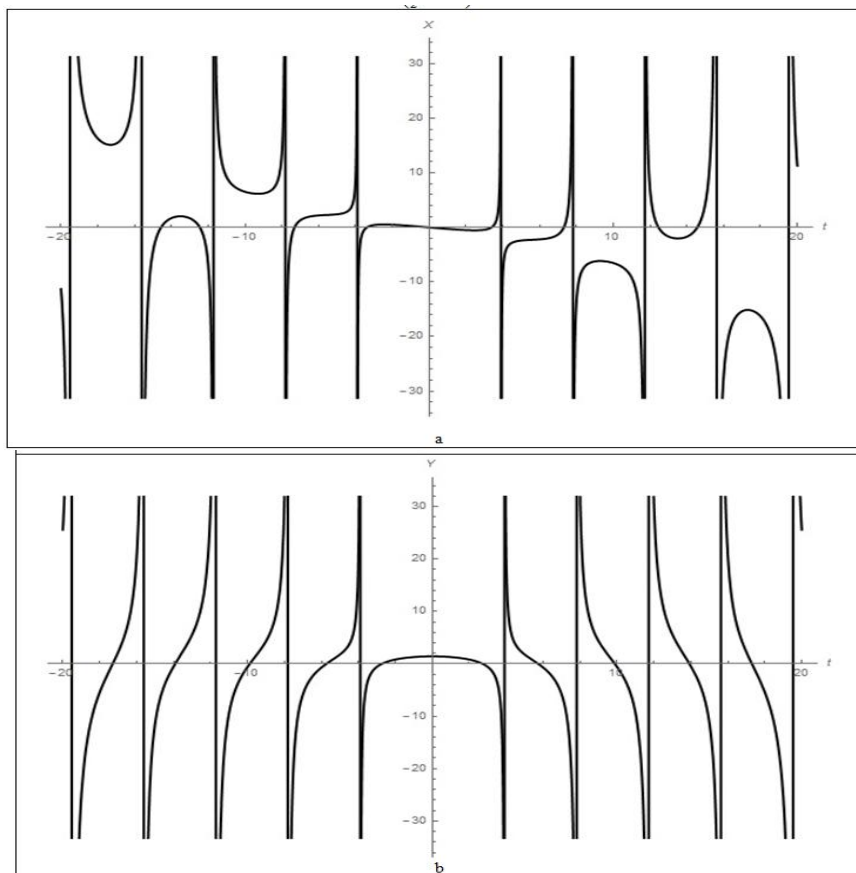


Fig. 10. Functions  $x_5(t)$  (a) and  $y_5(t)$  (b), belonging to Riemannian family of functions, which is determined by formulas (15).

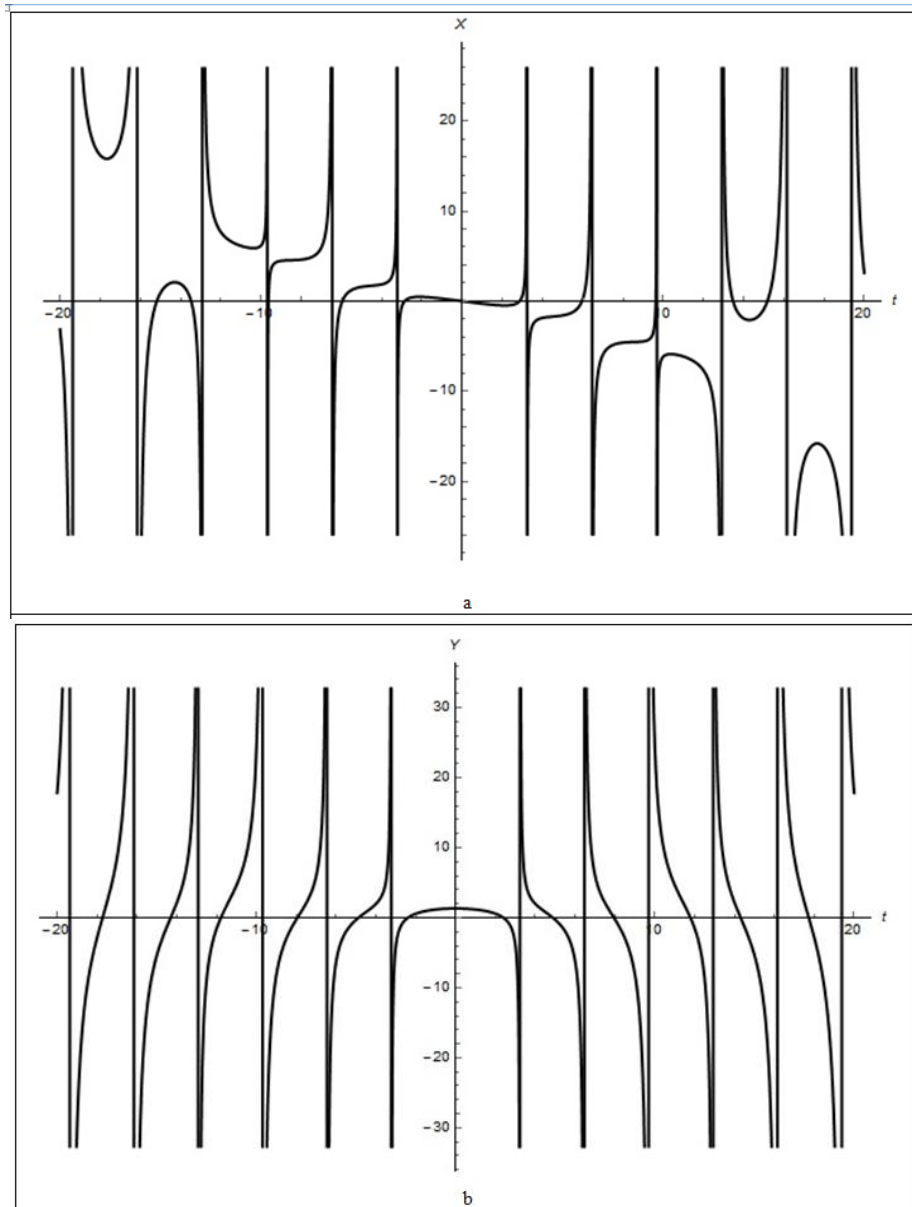


Fig. 11. Functions  $x_7(t)$  (a) and  $y_7(t)$  (b), belonging to Riemannian family of functions, which is determined by formulas (15).

The functions  $x_N(t)$  and  $y_N(t)$  of this Riemannian family for some values of  $N$  are shown in Fig. 10 and Fig. 11.

On the plane  $\{x, y\}$  each curve belonging to this Riemannian family of curves described parametrically by formulas (15), for each fixed value of  $N$  consists of a countable set of branches symmetric with respect to the  $y$  axis. These branches can be numbered with the help of an integer parameter  $m \geq 1$ , which specifies the position of asymptotes of infinite branches at  $t = t_m = \frac{2\pi m}{\ln N}$ .

The first branch for any value of  $N$  – i.e. a curve of the form  $x = x_{N,1}(t) \quad |t| < t_1$ , – is a continuous loop-shaped curve reminiscent of "the folium of Descartes" in some sense [4]. These loop-like curves form an infinite family of curves, which may be appropriately called "the foliatura of Descartes-Riemann". The Descartes-Riemann folium for  $N=5$  is shown in Fig. 12.

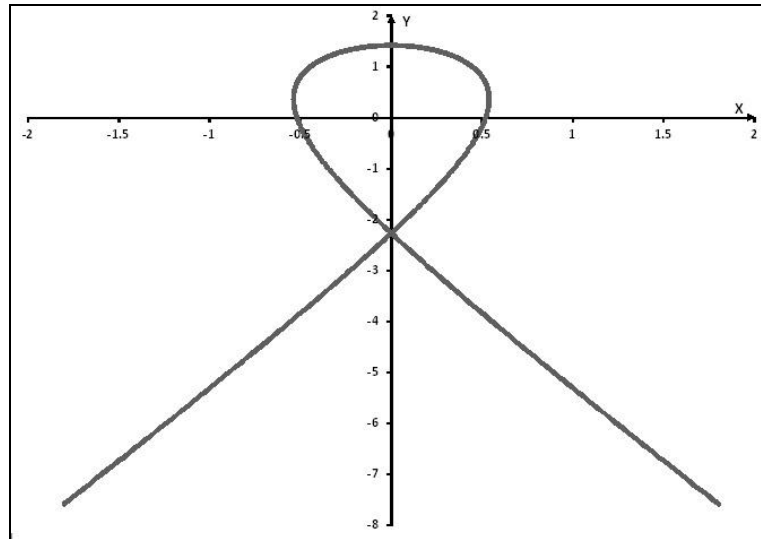


Fig. 12. The folium of Descartes-Riemann at  $N=5$ :  $x = x_{5,1}(t)$ .

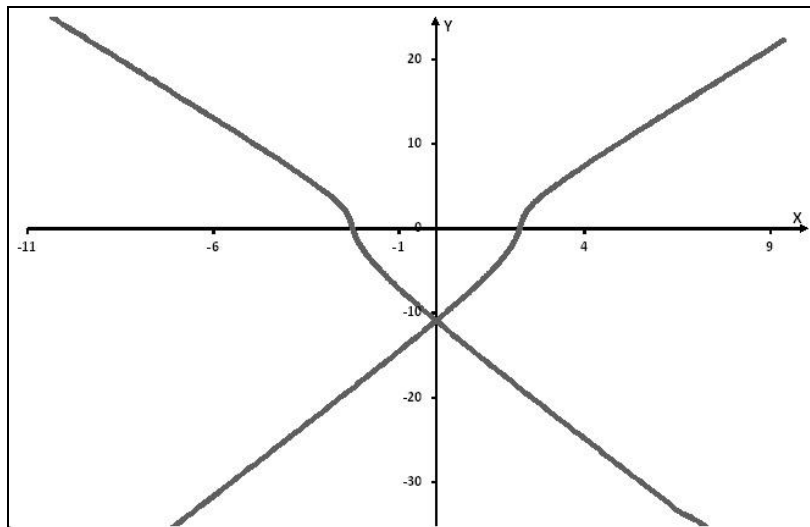


Fig. 13. The Riemann's fulguris at  $N=5$ :  $x = x_{5,2}(t)$ .

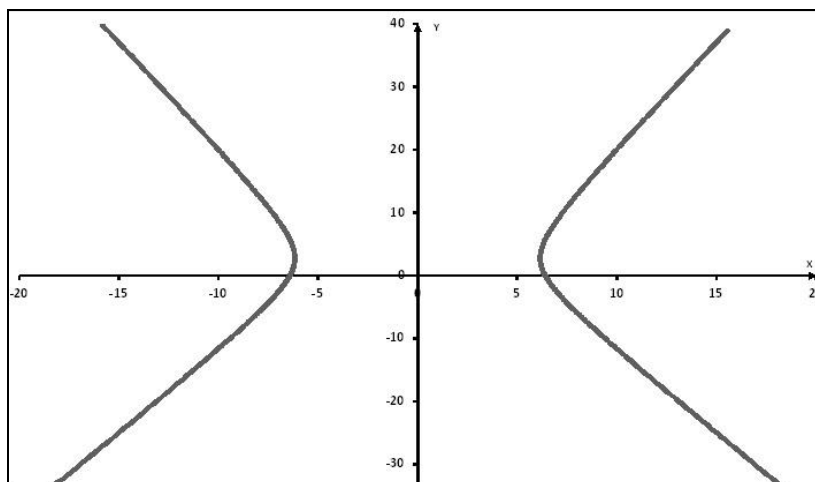


Fig. 14. The non-intersecting Riemann hyperbolas for  $N=5$ :  $x = x_{5,3}(t)$ .

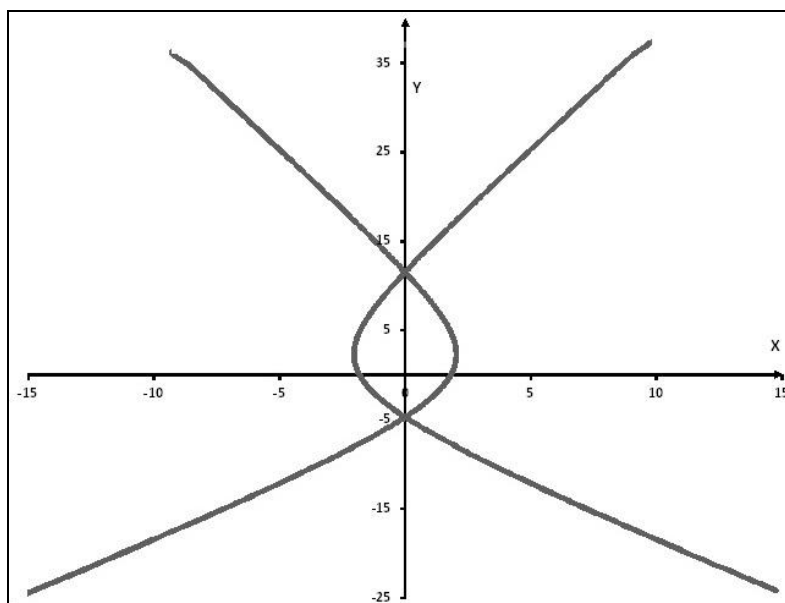


Fig. 15. The intersecting Riemann hyperbolas for  $N=5$ :  $x = x_{5,4}(t)$ .

All other branches of this two-index Riemann family  $x_{N,m}(t)$ ,  $m \geq 2$  are doubly-connected curves. From the point of view of geometric classification, they belong to three types of curves. The first type is curves having the form of a pair of symmetrical intersecting forked lightning curves ("Riemann's lightning" or "Riemann's fulguris"). One such "fulgur" is shown in Fig. 13. The second and third types of curves are hyperboloid curves ("Riemann hyperbolas") that do not have intersection points (see Figure 14), or have intersection points (see Figure 15). Each of the curves of the two-index Riemann family  $x_{N,m}(t)$  (15), ( $N \geq 3, m \geq 2$ ) is defined on two symmetric intervals with respect to the argument  $t: t_{m-1} < |t| < t_m$ . All these curves of the Riemannian family  $x_{N,m}(t)$ , are, of course, very far from the Riemann zeta function, but, in a sense, by their mode of introduction, they are genetically related to the function  $D$  (see formula (1)), – and, consequently, with the Riemann zeta function.

### VIII. Concluding Remark

Concluding this paper, we note that the "zeta effect" discovered here by us undoubtedly deserves a more thorough mathematical study. In a sense, it is related to the well-known "Gibbs phenomenon" [5], a parasitic oscillation of finite segments of the Fourier series near the point of discontinuity of the function. But the Gibbs phenomenon is localized near the point of discontinuity of the function. The zeta effect that we discovered is non-localized, it introduces parasitic noise for all values of the argument. The nature of the zeta effect is undoubtedly associated with a slow (logarithmic) change in the frequency of the harmonics in the Riemann series (9).

### References

- [1] M. Abramowitz, I Stegun, Handbook of Mathematical Functions with Formulas, Graphs, and Mathematical Tables (Martino Fine Books, 2014).
- [2] J. Borwein, D.M. Bradley, R. Crandall, Computational Strategies for the Riemann Zeta Function, J. Comp. App. Math. 121 (1–2): 2000, 247–296. URL: <http://empslocal.ex.ac.uk/people/staff/mrwatkin/zeta/borwein1.pdf>
- [3] E. Jahnke, F. Emde, F. Lösch, Tafeln höherer Funktionen / Sechste Aufgabe. Neubearbeitet von F. Lösch / B.D. Teubner (Verlagsgesellschaft, Stuttgart, 1960).
- [4] E.W. Weisstein, Folium of Descartes (From MathWorld). A Wolfram Web Resource. URL: <http://mathworld.wolfram.com/FoliumofDescartes.html>
- [5] E.W. Weisstein, Gibbs Phenomenon (From MathWorld). A Wolfram Web Resource. URL: <http://mathworld.wolfram.com/GibbsPhenomenon.html>